15TH IEA HEAT PUMP CONFERENCE
MAY 26–29, 2026 | HOFBURG
VIENNA 2026
DECARBONISATION THROUGH INNOVATION

Research on Performance of Transcritical CO_2 Heat Pump System with Distributed Compression

Junrui Nie, Lei Wang, Guoyuan Ma*, Yuexuan Gong, Fuping Li

Beijing university of technology, Beijing, 100124, China

Abstract

CO_2 heat pump system is one of advancing low-carbon heating technologies, of which performance optimization is helpful to enlarging its application, and the distributed compression system with stepped compression processes can effectively improve the energy efficiency ratio of transcritical CO_2 heat pump systems. This paper employs distributed compression cycle theory to construct a model of a transcritical CO_2 heat pump system. Through numerical simulation, the effects of key thermodynamic parameters—such as cycle temperatures and pressures—on system performance are analyzed. An exhaustive search method is applied to derive correlations between the optimal intermediate pressure and the system's key thermodynamic parameters. The results indicate that the optimal intermediate pressure in the distributed compression cycle is related to the evaporation temperature, final discharge pressure, and gas cooler outlet temperature. The fitted multivariate correlation achieves a coefficient of determination (R^2) of 0.8899. Furthermore, the system performance surpasses that of single-stage transcritical CO_2 systems (including those with internal heat exchanger or ejector) and some two-stage systems. This study validates the feasibility of the distributed compression technology and provides theoretical support for the design of high-efficiency transcritical CO_2 heat pump systems.

Keywords: CO_2 heat pump system; distributed compression system; transcritical cycle; Performance optimization ;

1. Introduction

Driven by global climate governance and energy transition, low-carbon heating technologies in the building sector have become crucial for achieving carbon neutrality goals. The International Energy Agency, in "The Future of Heat Pumps 2023," explicitly states that heat pump technology, with its high energy efficiency ratio, could reduce global building carbon emissions by over 50% before 2050 [1]. As a natural working fluid, CO_2 (R744) is recognized as an innovative alternative to fluorinated refrigerants due to its 0 ODP, GWP of 1, and stable performance under high-temperature conditions [2]. However, single-stage transcritical CO_2 heat pump systems face several thermodynamic challenges in commercialization: nonlinear, abrupt changes in working fluid properties within the supercritical region lead to a sharp rise in compressor power consumption [3]; a mismatch between gas cooler outlet temperature and user-side demand results in irreversible heat transfer losses [4]; and significant performance degradation in low-temperature environments (below -30°C) [5].

In recent years, cycle structure innovation has become a core direction for improving the performance of transcritical CO_2 heat pumps. However, traditional multi-stage compression technology is still limited to optimization in the gaseous superheat region and fails to effectively utilize the adjustable properties of supercritical CO_2 for thermodynamic cycle reconstruction [6]. In the field of cycle structure innovation, regenerative technology, which recovers waste heat from the working fluid before expansion through an internal heat exchanger, has been proven to increase system heating capacity by 10%-20% [7]. Although existing research has promoted the development of transcritical CO_2 heat pump technology in many aspects, its energy efficiency improvement still faces challenges: neglecting the potential of adjustable working fluid properties in the supercritical region for thermodynamic cycle reconstruction [8]. Wang et al. [9] proposed a novel concept of

*Guoyuan Ma. Tel.: 010-67391613
E-mail address: magy@bjut.edu.cn

secondary pressurization of CO_2 in the transcritical region of the traditional single-stage compression cycle, termed the distributed compression cycle.

This research investigates the application of distributed compression cycle technology in transcritical CO_2 heat pumps. Its technological breakthrough is mainly reflected in: systematically reducing the working fluid enthalpy before throttling through stepwise secondary pressurization and stepped heat release processes, significantly enhancing the heating capacity per unit mass of the working fluid; establishing a mathematical model of the distributed compression cycle, revealing the coupling mechanism of key parameters such as intermediate pressure, discharge pressure, and temperature, providing an important theoretical basis for the development of a new generation of high-efficiency heat pump systems.

2. System Principle

The schematic diagram of the distributed compression system is depicted in Fig.1. The distributed compression refrigeration cycle differs from conventional transcritical CO_2 compression cycles in that the supercritical CO_2 exiting the gas cooler after the first compression undergoes a secondary pressurize process. The supercritical CO_2 from the secondary pressurize is then cooled by a second gas cooler, with the CO_2 outlet temperature from gas cooler 2 identical to that of gas cooler 1. Both gas coolers can absorb the heat released by the supercritical CO_2 at precisely the same heat sink temperature.

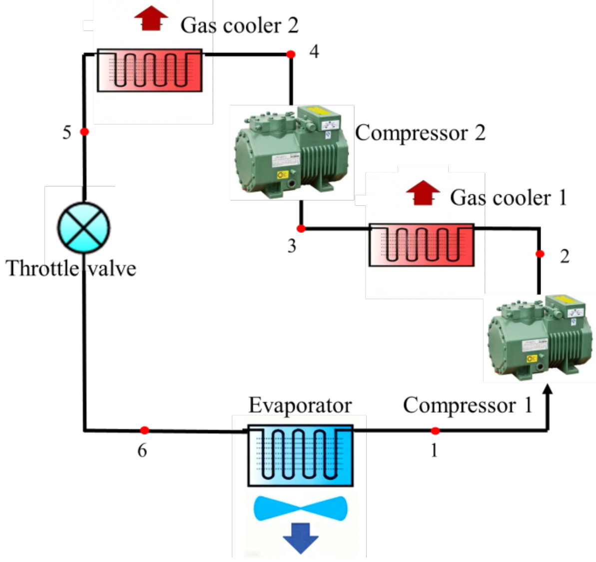

Figure 1. Schematic diagram of the transcritical distributed compression system

The complete CO_2 transcritical distributed compression cycle is represented on the P-h diagram in Fig. 2 as 1-2-3-4-5-6-1. Segments 1-2 denote the compressor's initial compression process of CO_2 from the evaporator. Segments 2-3 represent the cooling process of the initially compressed CO_2 in the gas cooler. Under conventional heat sink conditions and without any subcooling methods, the CO_2 is cooled to state point 3. An isothermal line at state point 3 is depicted in Fig. 2, where point 3 represents a supercritical state. Segment 3-4 signifies the secondary pressurization process of the supercritical CO_2 cooled to state point 3, where the temperature and pressure of the supercritical CO_2 are further increased to reach state point 4. Segment 4-5 represents the cooling of the supercritical CO_2 at state point 4 under the same heat sink conditions as the 2-3 process, resulting in state point 5 having the same temperature as state point 3. Segments 5-6 represent the throttling process of CO_2 to generate a cooling effect. Lastly, the segment 6-1 represents the heat absorption process of CO_2 in the evaporator. In Fig.2, 1-2-3-7-1 and 1-2-3'-7'-1 represent the baseline CO_2 transcritical cycle process and the CO_2 transcritical cycle process with subcooling to state point 3'.

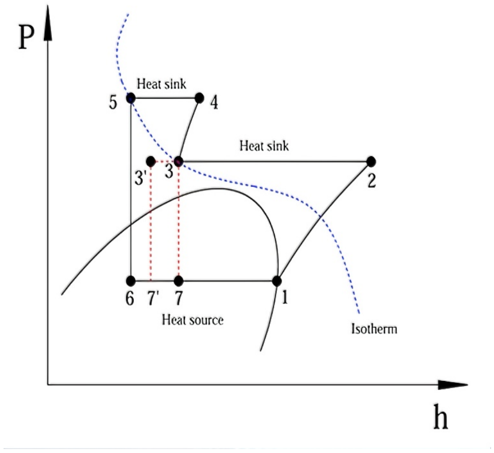

Figure 2． P-h diagram of the distributed compression cycle.

The distributed compression system employs two pressurize and two heat release configurations, conceptually similar to the traditional two stage compression system cycle. However, there are fundamental differences between the distributed and two-stage compression systems regarding the location of the second pressurize and heat release processes and the ultimate thermodynamic objectives. The second pressurize stage in the distributed compression system occurs within the supercritical region, whereas in the two-stage compression cycle, it occurs in the cycle's superheated gas region. The objective of the distributed compression system is to achieve enhanced heat transfer of supercritical CO_2 under original heat sink conditions through the second pressurize and heat release stages, thereby reducing the enthalpy of CO_2 prior to throttling and ultimately enhancing the unit refrigeration and heating capacity. In contrast, the primary goal of the two-stage compression cycle is to minimize irreversible losses during the compression process.

3. Methods

In the heating operating condition, for a distributed compression transcritical CO_2 cycle, the heating capacity is:

$$\dot{Q}_{DC} = \dot{m}[(h_2 - h_3) + (h_4 - h_5) \tag{1}$$

The power input of the DC transcritical CO_2 cycle is the sum of the power input required for two parts of the pressure boost process. The cyclic power input is

$$\dot{W}_{DC} = \dot{m}[(h_2 - h_1) + (h_4 - h_3)] \tag{2}$$

When considering the isentropic efficiency of the compressor, the enthalpy values at state points 2 and 4 change accordingly, leading to adjustments in the actual system power consumption, heating capacity, and COP. The isentropic efficiency is primarily influenced by the compressor suction and discharge pressures and can be approximated by the following equation [10].

$$\eta_{is1} = 0.8014 - 0.04842\frac{P_{gc}}{P} \tag{3}$$

$$\eta_{is2} = 0.8014 - 0.04842\frac{P}{P_e} \tag{4}$$

The COP is:

$$COP_{DCS} = \frac{\dot{Q}_{DCS}}{\dot{W}_{DCS}} = \frac{(h_2-h_3)+(h_4-h_5)}{(h_2-h_1)+(h_4-h_3)} \tag{5}$$

For the basic transcritical CO_2 heat pump cycle, the COP is:

$$COP_C = \frac{\dot{Q}_C}{\dot{W}_C} = \frac{(h_2 - h_3)}{(h_2 - h_1)} \quad (6)$$

It can be assumed that a coefficient of performance represents the benefit of the secondary boost process to the whole refrigeration system, expressed in the COP_Z.

$$COP_Z = \frac{(h_4 - h_5)}{(h_4 - h_3)} \quad (7)$$

So there may be three mathematical relationships as follows:

a. When $COP_Z = COP_C$, Then $COP_{DCS} = COP_C$

b. When $COP_Z > COP_C$, Then $COP_{DCS} > COP_C$

c. When $COP_Z < COP_C$, Then $COP_{DCS} < COP_C$

If the isentropic efficiencies of the two pressurization processes are similar, the physical properties of CO_2 determine that for the same pressure change, the isentropic line at state point 3 is steeper than that at state point 1. This means the CO_2 cycle has higher compression efficiency, requiring less energy to compress per unit mass of CO_2. Wang Lei et al., using the pressure-enthalpy diagram and similarity principle, concluded that $COP_Z > COP_C$ fully exists [9]. This principle proves that even though the secondary pressurization process increases the overall power input of the system compared to the basic system, it can still improve the system COP.

Numerical calculations are employed to analyze the system cycle under varying key parameters. The selected numerical calculation conditions are outlined in Table 1. By sequentially varying the set evaporation temperature, gas cooler outlet temperature, and final discharge pressure, an exhaustion method is used to calculate the COP of the system under different intermediate pressures. The intermediate pressure corresponding to the maximum COP is considered the optimal intermediate pressure under that operating condition. Mathematical fitting methods are then applied to derive a correlation for the optimal intermediate pressure of the distributed system, which is related to the evaporation temperature, gas cooler outlet temperature, and final discharge pressure.

Table 1 Calculated conditions

Variable parameters	Operating conditions range
Temperature at gas cooler outlet (°C)	32.5、35、37.5、40、42.5、45
Evaporation temperature (°C)	-20、-15、-10、-5、0、5、10
Discharge pressure (MPa)	10、10.5、11、12、13、14
Intermediate pressure (MPa)	7.4~

4. Results Analysis

Figure 3 shows that under different final discharge pressure conditions, the system COP exhibits a unimodal distribution characteristic with the increase of intermediate pressure, i.e., it rises first and then declines, and each discharge pressure corresponds to a unique optimal intermediate pressure. When the intermediate pressure is low, the thermodynamic compatibility between the secondary pressurization and the two-stage heat release is insufficient. As the intermediate pressure gradually increases, the isentropic efficiencies of the two-stage compression process are synergistically optimized, irreversible losses in the system decrease, and COP continuously improves. When the intermediate pressure exceeds the optimal value, the increase in irreversible losses in the high-pressure side compression process outweighs the improvement in heating capacity, leading to a decline in COP. Meanwhile, the discharge pressure indirectly regulates the adaptation range of the optimal intermediate pressure by altering the enthalpy change characteristics of supercritical CO_2.

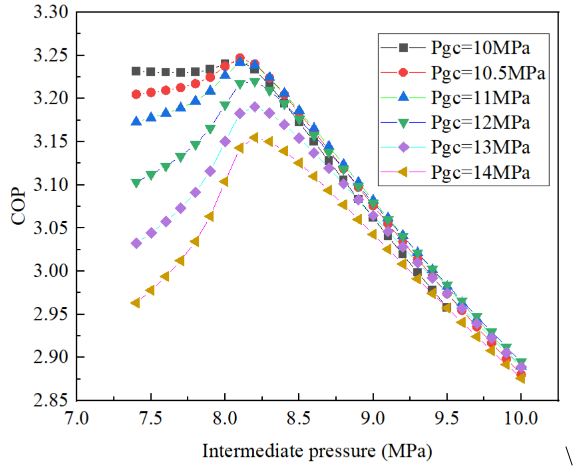

Figure 3. Variation of COP with intermediate pressure under different exhaust pressures

Figure 4 shows that as the gas cooler outlet temperature increases, the peak COP of the system decreases, and the optimal intermediate pressure shifts toward a higher range. Under all gas cooler outlet temperature conditions, the COP follows a trend of first increasing and then decreasing. A higher gas cooler outlet temperature directly increases the pre-throttling enthalpy of CO_2, intensifying throttling losses. At lower intermediate pressures, the two-stage heat release process cannot effectively reduce the pre-throttling enthalpy, resulting in poor system performance. As the intermediate pressure increases, the heat rejection intensity after the second-stage compression strengthens, significantly reducing throttling losses and allowing the COP to gradually rise to its peak. Higher gas cooler outlet temperatures require higher intermediate pressures to balance the thermodynamic matching between the two-stage compression and heat rejection processes, leading to a shift in the optimal intermediate pressure and an overall reduction in COP due to the accumulation of irreversible losses.

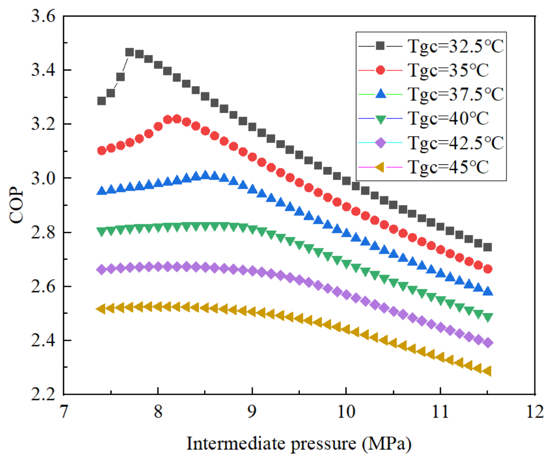

Figure 4. Variation of COP with intermediate pressure at different gas cooler outlet temperatures

Figure 5 shows that as the evaporation temperature increases, the peak COP of the system becomes higher, and the distribution range of the optimal intermediate pressure corresponding to each evaporation temperature is relatively concentrated. In all cases, the COP exhibits a unimodal variation with intermediate pressure. This occurs because a higher evaporation temperature increases the CO_2 evaporation pressure and suction enthalpy, thereby reducing the suction-side irreversible losses and compression work of the first-stage compressor. When the intermediate pressure falls within the suitable range, the isentropic efficiencies of the two-stage compression process are synergistically optimized, maximizing the ratio of heating capacity to power consumption. Meanwhile, the optimal intermediate pressure is mainly determined by the enthalpy variation characteristics of supercritical CO_2 and the matching requirements of the two-stage cycle, and is less affected by the evaporation temperature. Thus, the optimal intermediate pressure range remains relatively concentrated across different evaporation temperature conditions.

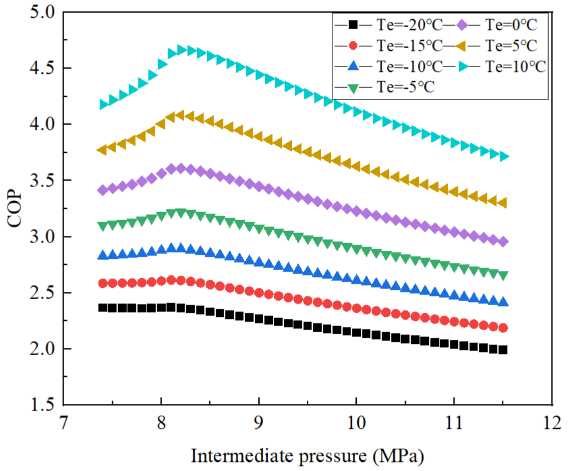

Figure 5. Variation of COP with intermediate pressure at different evaporation temperatures

The three subplots in Figure 6 elucidate the influence of key parameters on the optimal intermediate pressure: (a) As the evaporation temperature rises from -20°C to 0°C, the optimal intermediate pressure gradually increases from 7.4 MPa to 8.2 MPa and then stabilizes with further increases in evaporation temperature; (b) The optimal intermediate pressure exhibits a monotonically increasing trend with rising final discharge pressure, climbing from 7.4 MPa to 8.3 MPa as the exhaust pressure increases from 10 MPa to 14 MPa; (c) The optimal intermediate pressure continuously rises with increasing gas cooler outlet temperature, increasing from 7.4 MPa to 8.8 MPa as the gas cooler outlet temperature rises from 35°C to 45°C. This indicates that the optimal intermediate pressure is simultaneously influenced by evaporation temperature, gas cooler outlet temperature, and final discharge pressure

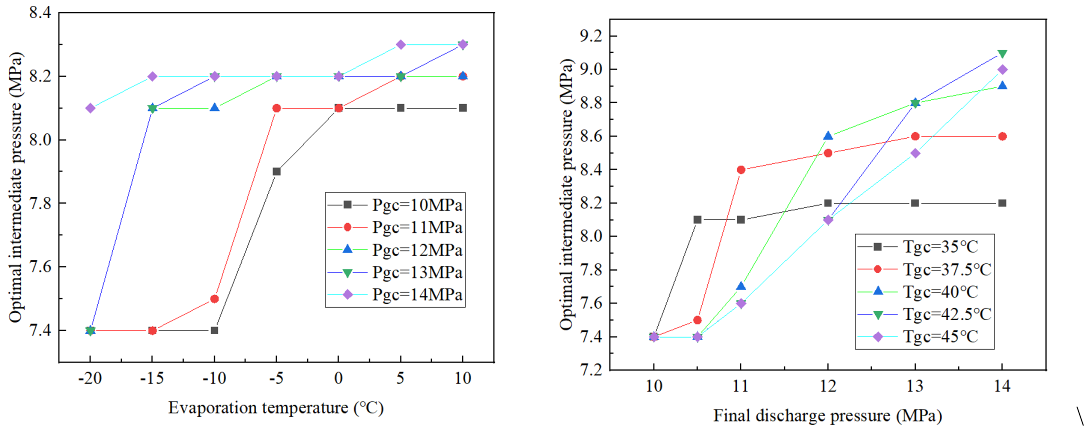

(a) Evaporation temperature

(b) Final discharge pressure

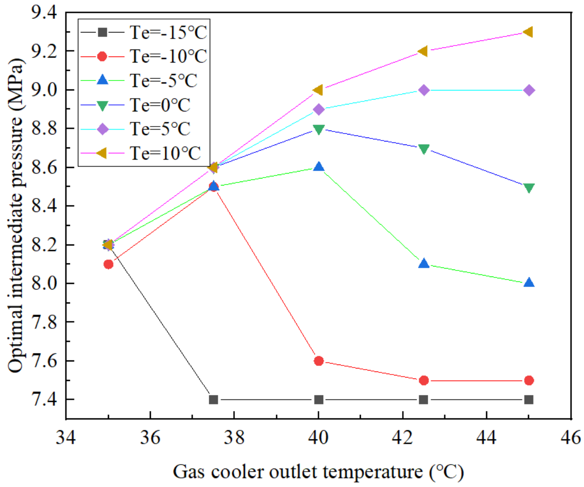

(c) Gas cooler outlet temperature

Figure 6. Effect of system parameters on the optimal intermediate pressure

Based on the findings regarding the variation patterns of the optimal intermediate pressure with evaporation temperature, gas cooler outlet temperature, and final discharge pressure, it is concluded that the correlation formula for the optimal intermediate pressure is jointly determined by these three parameters: evaporation temperature, gas cooler outlet temperature, and final discharge pressure. Employing a multivariate regression method to construct the correlation formula for the optimal intermediate pressure, the resulting expression for the optimal intermediate pressure is as follows:

$$\begin{aligned} P_{mid} = {} & 36.125062 - 3.657836 \times T_e - 8.818544 \times P_{gc} + 0.003872 \times T_{gc} - 0.001841 \times T_e^2 + \\ & 0.053113 \times T_{gc}^2 - 0.000164 \times T_e P_{gc}^2 - 0.005990 \times T_e P_{gc} T_{gc} - 0.000610 \times T_e T_{gc}^2 - \\ & 0.007221 \times P_{gc}^3 + 0.003757 \times P_{gc}^2 T_{gc} - 0.006263 \times P_{gc} T_{gc}^2 + 0.000997 \times T_{gc}^3 \end{aligned} \tag{8}$$

Eq. (8) achieves a coefficient of determination (R^2) of 0.8899.

Table 2 presents a performance comparison between the distributed transcritical CO_2 compression heat pump system proposed in this study and various other transcritical CO_2 system configurations, with the COP serving as the core thermodynamic evaluation metric. The distributed system demonstrates performance advantages over single-stage transcritical CO_2 systems (including configurations assisted by internal heat exchangers, ejectors, or a combination of both) as well as two-stage transcritical CO_2 systems incorporating flash tanks or parallel compression-ejector assistance. In contrast, its performance is slightly inferior to that of two-stage transcritical CO_2 systems equipped with internal heat exchangers, single-stage systems integrating DMS, thermoelectric-heat exchangers, or novel adjustable vortex tube expansion devices, and two-stage systems combining vortex tubes with DMS-internal heat exchangers. Subsequent adoption of auxiliary devices or configuration optimizations that can significantly enhance transcritical CO_2 cycle performance may offer potential for further improvement in the distributed system's performance.

Table 2 Comparison of the performance of the transcritical distributed compression system with other systems

Evaporating Temperature(°C)	Gas cooler outlet temperature(°C)	Discharge Pressure(MPa)	Characteristics	COP	COP_{DCS} (System in the same working Condition)	ΔCOP to Reference system (%)
0	30	7.7	Single-stage + IHX[18]	3.21	4.31	34.27
10	30	13	Single-stage + Ejector[19]	4	4.36	9.00
10	30	11.75	Single-stage + IHX + ejector[19]	4.29	4.53	5.59

-15	35	8.5	Two-stage + IHX[17]	2.54	2.52	-0.79
-5	45	13	Single-stage + DMS[12]	2.81	2.53	-9.96
20	55	13	Single-stage + TEG-IHX[11]	3	2.71	-9.67
-10	35	8.96	Two-stage + Flash tank[20]	2.366	2.84	20.03
-15	40	11	Single-stage + Vortex tube.[15]	2.21	2.32	4.98
-5	50	11	Single-stage +a novel adjustable vortex tube expansion[16]	2.53	2.04	-19.37
-15	40	11	Two-stage + Vortex tube[15]	2.75	2.32	-15.64
-10	35	9	Two-stage + DMS+ IHX[14]	3.13	2.86	-8.63
-15	45	10.8	Two-stage + PC + ejector[13]	1.64	2.09	27.44

5. Conclusion

Improving transcritical CO_2 vapor compression system performance has always been a research hotspot. Breaking through the conventional approach of secondary release heat at a higher pressure can also reduce the enthalpy value of CO_2 after throttling, achieving an improvement in system performance. The proposal of the DC cycle provides a new way for performance improvement, and the following conclusions are drawn as follows:

(1) There exists an optimal intermediate pressure in the transcritical distributed compression system. Its value first increases and then stabilizes with rising evaporation temperature, and increases monotonically with increasing final discharge pressure and gas cooler outlet temperature. This behavior originates from the enthalpy change characteristics of supercritical CO_2 and the thermodynamic matching requirement for two-stage compression and heat rejection.

(2) A multivariate cubic polynomial correlation for the optimal intermediate pressure, constructed based on numerical simulation data, achieves a coefficient of determination (R^2) of 0.8899. It accurately reflects the synergistic effects of evaporation temperature, gas cooler outlet temperature, and final discharge pressure, providing a reliable calculation tool for engineering design.

(3) Performance comparisons indicate that this system demonstrates superior thermodynamic performance compared to single-stage systems (including those with internal heat exchangers, ejectors, or their combination) and two-stage transcritical CO_2 systems equipped with flash tanks or parallel compression-ejector configurations. However, it is slightly outperformed by systems integrating specialized devices or novel vortex tubes.

By adopting an innovative architecture featuring two-stage compression and heat rejection within the supercritical region, this system effectively reduces the pre-throttling enthalpy. This approach transcends the conventional optimization constraints of multi-stage compression, thereby establishing a theoretical foundation for the development of next-generation, high-efficiency, low-carbon heat pump technologies. Subsequent performance enhancements can be pursued through the integration of auxiliary devices.

References

[1]. IEA. The future of heat pumps 2023. Paris: OECD/IEA; 2023.

[2]. Ma Y, et al. Natural refrigerants for decarbonization: a critical review of CO_2 limits and opportunities. Renew Sustain Energy Rev 2022;168:112791.

[3]. Bellos E, et al. Supercritical CO_2 thermodynamic anomalies in transcritical cycles: a machine learning approach. Energy Convers Manag 2023;275:116473.

[4]. Wu Z, et al. Dynamic temperature matching for CO_2 heat pumps using adaptive control. Appl Therm Eng 2021;195:117201.

[5]. Dai B, et al. Extreme cold climate operation of CO_2 heat pumps: a comprehensive review. Energy 2023;263:12567.

[6]. Liu X, et al. Phase-change thermal storage integrated CO_2 heat pumps for load shifting. Appl Energy 2022;306:118101.

[7]. Yang J, et al. Performance analysis of CO_2 heat pump with internal heat exchanger. Energy 2015;87:453-462.

[8]. Llopis R, et al. Limitations of conventional multi-stage compression in transcritical CO_2 systems. Energy Convers Manag 2021;243:114367.

[9]. Wang L, Zhang Y, Ma G. Theoretical investigation of a novel distributed compression cycle for CO_2 transcritical system. Energy Build 2024;304:113853.

[10]. Wang SG, Tuo HF, Cao F, et al. Experimental investigation on air-source transcritical CO_2 heat pump water heater system at a fixed water inlet temperature. Int J Refrig 2013;36(3):701-716.

[11]. Kwan TH, Shen Y, Wu Z, et al. Performance analysis of the thermoelectric device as the internal heat exchanger of the transcritical CO_2 cycle. Energy Convers Manag 2020;208:112585.

[12]. He YJ, Cheng JH, Chang MM, et al. Modified transcritical CO_2 heat pump system with new water flow configuration for residential space heating. Energy Convers Manag 2021;230:113791.

[13]. Ye AQ. Performance study on air-source transcritical CO_2 heat pump heating system with ejector parallel compression. Harbin: Harbin Institute of Technology; 2022. https://doi.org/10.27061/d.cnki.ghgdu.2022.002250.

[14]. Huang S, Xiang XY, Li A, Jin X, A Runa, Zhang JP. Cycle optimization and environmental-economic evaluation of transcritical CO_2 heat pump heating system. Integr Intell Energy 2025. https://link.cnki.net/urlid/41.1461.TK.20251128.1652.004.

[15]. Wu FM, Li SQ, Li JF, et al. Optimization technology of CO_2 transcritical cycle heat pump in severe cold conditions. Adv New Renew Energy 2023;11(3):255-263.

[16]. Liu YF, Yu Y, Zhang H, et al. Performance study on a novel transcritical CO_2 heat pump system with adjustable vortex tube expansion. HVAC 2024;54(12):128-133.

[17]. Cecchinato L, Chiarello M, Corradi M, et al. Thermodynamic analysis of different two-stage transcritical CO_2 cycles. Int J Refrig 2009;32(5):1058-1067.

[18]. Lu DX, Song X, Lei Q, et al. Experimental study on heating performance of CO_2 train heat pump system with regenerator under low temperature conditions. Refrigeration Technol 2023;43(1):30-36.

[19]. Li WQ, Yue B, Zhang H, et al. Cycle optimization and maximum heating temperature research of transcritical CO_2heat pump. J Eng Thermophys 2025;46(11):3506-3515.

[20]. Wang Q, Zhang J, Bi SH. Energy efficiency analysis of steam ejector transcritical CO_2 refrigeration system. Refriger Air Cond 2025;1-6. https://doi.org/10.20245/j.issn.1009-8402.2025.12.007.